Int. J. Heat Mass Transfer. Vol. 29, No. 12, pp. 1979–1988, 1986
Printed in Great Britain

0017-9310/86 $3.00+0.00
Pergamon Journals Ltd.

Conjugate natural convection in a square enclosure: effect of conduction in one of the vertical walls

D. A. KAMINSKI and C. PRAKASH*

Department of Mechanical Engineering, Aeronautical Engineering & Mechanics, Rensselaer Polytechnic Institute, Troy, NY 12180–3590, U.S.A.

(*Received* 22 *July* 1985 *and in final form* 15 *April* 1986)

Abstract—Steady, laminar, natural convection flow in a square enclosure has been analysed numerically. One vertical wall of the enclosure is thick, with a finite thermal conductivity, while the other three walls are taken to be of zero thickness. The problem is conjugate and the main focus of the study is on examining the effect of conduction in the wall on the natural convection flow in the enclosure. Three separate models to account for the wall conduction are investigated: (i) the complete conjugate case in which conduction in the thick vertical wall is assumed to be fully two-dimensional; (ii) a one-dimensional model in which conduction in the wall is assumed to be in the horizontal direction only; and (iii) a lumped parameter approach which assumes the solid–fluid interface temperature to be uniform. A Boussinesq fluid with Prandtl number of 0.7 (air) and Grashof numbers ranging from 10^3 to 10^7 are considered. For Grashof number $>10^5$, the temperature distribution in the wall shows significant two-dimensional effects and the solid–fluid interface temperature is found to be quite non-uniform. This non-uniformity tends to make the flow pattern in the enclosure asymmetric. In the parametric range investigated, all three models predict nearly the same value for the overall heat transfer.

INTRODUCTION

The problem analysed

Steady, laminar, natural convection flow in a square enclosure has been analysed. The configuration is sketched in Fig. 1. Three walls of the enclosure are assumed to be of zero thickness while the fourth, the right vertical wall, has a thickness t. The horizontal walls are insulated, the left vertical face is at a uniform temperature T_C, and the right edge is isothermal at a temperature T_H. The problem is conjugate and the goal of the analysis is to solve numerically for the natural convection flow in the enclosure taking account of the conduction in the right vertical wall.

Motivation

Natural convection in enclosures is a topic of considerable engineering interest. Applications range from thermal design of buildings, to cryogenic storage, furnace design, nuclear reactor design, and others. Several comprehensive reviews of the literature have been published [1–3].

The problem of natural convection flow in a rectangular enclosure with uniform temperature at the side walls and insulated top and bottom walls has been the subject of many earlier studies. Elder [4, 5] performed a comprehensive set of flow visualization experiments which delineated the flow regimes for this geometry. Early numerical studies were published by Wilkes [6], followed by Gershuni *et al.* [7] and de Vahl Davis [8]. Recently, Jones [9] has published a very detailed comparison of experimental and numerical results; in all cases, the agreement between the two is very good, validating the numerical methods of studying this type of problem.

In the studies cited above, the walls of the enclosure are assumed to be of zero thickness and conduction in the walls is not accounted for. However, in many practical situations, especially those concerned with the design of thermal insulation, conduction in the walls can have an important effect on the natural convection flow in the enclosure; it is this recognition that constitutes the motivation for the present study.

Literature on conjugate problems is sparse. The configuration discussed in this paper has been studied before by Lauriat [10]; in fact, in terms of Lauriat's work, the present study corresponds to $A = 1$, $N_r = 0$, and $B_i = \infty$. The essential differences in the two investigations are: (i) the one-dimensional wall conduction

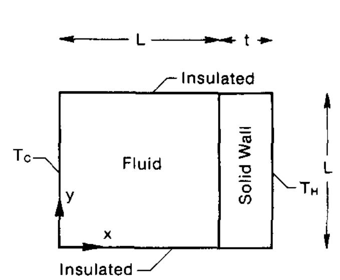

FIG. 1. Schematics of the problem analysed.

*Present address: CHAM of North America, Inc., 1525-A Sparkman Drive, Huntsville, AL 35805, U.S.A.

NOMENCLATURE

c_p	specific heat of the fluid
Gr	Grashof number, $g\beta(T_H - T_C)L^3/\nu^2$
g	acceleration due to gravity
k	thermal conductivity of the fluid
k_w	thermal conductivity of the solid wall
L	length of side of the square enclosure
Nu	overall Nusselt number, $Q/k(T_H - T_C)$
P	dimensionless pressure, $(p+\rho gy)/\rho(\nu/L)^2$
Pr	Prandtl number of the fluid, $\mu c_p/k$
p	pressure
Q	total heat transfer across the enclosure
q	local heat flux
t	thickness of the solid wall
T	temperature
T_C	temperature of the left vertical side
T_H	temperature of the right vertical side
U, V	dimensionless velocity components, $u/(\nu/L)$, $v/(\nu/L)$
u, v	velocity components
x, y	coordinates
X, Y	dimensionless coordinates, x/L, y/L.

Greek symbols

β	coefficient of thermal expansion of the fluid
θ	dimensionless temperature, $(T-T_C)/(T_H-T_C)$
μ	viscosity of the fluid
ν	kinematic viscosity of the fluid
ρ	density of the fluid
ψ_{max}	maximum value of the streamfunction in the enclosure.

model has been included in the present work for comparison; (ii) the variation of local heat flux at the solid–fluid interface has been examined; and (iii) a higher range of the Grashof number was investigated.

The effect of wall conduction on natural convection flow in an enclosure has also been examined by Balvanz and Kuehn [11]. They considered the case of volumetric heat generation within the wall, and the outer face of the thick wall was taken to be insulated. Larson and Viskanta [12] accounted for wall conduction effects in an enclosed fire problem. Only one-dimensional wall conduction was considered. In both of these studies, the problem definition and boundary conditions are different from those investigated in the present study.

More recently, Kim and Viskanta [13–15] have carried out a comprehensive experimental and numerical study of natural convection flow in an enclosure with conducting walls. They examined the case in which all four walls are conducting. Hence, their problem is different than the one investigated in this paper. In the present study, the choice to restrict to only one thick wall is intentional, the goal being to examine a simple effect in isolation; the numerical procedure used can, however, as easily handle the case in which all four walls are conducting.

The effect of wall conduction on natural convection in slots has also been examined by Mallinson [16]. Mallinson's study involves a three-dimensional slot, with the wall *parallel* to the plane of Fig. 1 being thick. In addition, the periodic boundary conditions are intended to simulate the case of a series of slots separated by thick wall partitions.

ANALYSIS

Assumptions

The flow in the enclosure is assumed to be two-dimensional with velocity components u and v along the x and y coordinates, respectively (see Fig. 1). All fluid properties are assumed constant, and the fluid is considered to be incompressible except for the buoyancy term which is computed using the Boussinesq-type equation of state. Viscous dissipation and compression work are neglected in the energy equation and so are the radiation effects.

Equations for the fluid part of the enclosure

In terms of dimensionless variables which are defined in the nomenclature, the flow is governed by the following set of conservation equations

$$\frac{\partial U}{\partial X}+\frac{\partial V}{\partial Y}=0 \tag{1}$$

$$U\left(\frac{\partial U}{\partial X}\right)+V\left(\frac{\partial U}{\partial Y}\right)=-\frac{\partial P}{\partial X}+\nabla^2 U \tag{2}$$

$$U\left(\frac{\partial V}{\partial X}\right)+V\left(\frac{\partial V}{\partial Y}\right)=-\frac{\partial P}{\partial Y}+Gr\theta+\nabla^2 V \tag{3}$$

$$U\left(\frac{\partial \theta}{\partial X}\right)+V\left(\frac{\partial \theta}{\partial Y}\right)=\left(\frac{1}{Pr}\right)\nabla^2\theta. \tag{4}$$

As for the boundary conditions, both the velocity components are zero at the walls. The dimensionless temperature θ is equal to zero at the left vertical wall while $\partial\theta/\partial Y = 0$ at the top and the bottom horizontal walls.

The complete conjugate case with two-dimensional wall conduction

In a complete analysis, the two-dimensional temperature distribution in the wall is governed by the heat conduction equation which, in dimensionless form, reads

$$\nabla^2\theta = 0. \tag{5}$$

At the right vertical edge, $\theta = 1$. At the solid–fluid interface, the temperature and the heat flux must be continuous. The latter condition is mathematically expressed as

$$\left(\frac{\partial\theta}{\partial X}\right)_{\text{fluid}} = \frac{k_w}{k}\left(\frac{\partial\theta}{\partial X}\right)_{\text{wall}} \quad \text{at } X = 1. \tag{6}$$

Equations (1)–(4), which determine the flow, are, therefore, coupled to equations (5) and (6) which describe the two-dimensional conduction in the wall.

One-dimensional wall conduction model

In the more commonly used one-dimensional wall conduction model, it is assumed that the heat flow in the wall is in the horizontal (x) direction only. This treatment can be mathematically described by saying $-k(\partial T/\partial x)_{\text{fluid}} = k_w(T-T_H)/t$, at the solid–fluid interface. In dimensionless terms this reads

$$-\left(\frac{\partial\theta}{\partial X}\right)_{\text{fluid}} = \left(\frac{k_w L}{kt}\right)(1-\theta) \quad \text{at } X = 1. \tag{7}$$

The advantage of using this model is that one does *not* have to solve any heat conduction equation in the wall; that is, only the flow equations, equations (1)–(4), are to be solved, and the effect of wall conduction is implied through the boundary condition expressed by equation (7) which is imposed at $X = 1$. This can provide a considerable saving in the computational effort.

Lumped parameter approach

The lumped parameter method* may be used to estimate the total heat transfer across the enclosure. Implicit in this treatment is the assumption that the solid–fluid interface is at a uniform temperature T_i. If this is the case, then the fluid is driven by an effective Grashof number Gr_C given by

$$Gr_C = \frac{g\beta(T_i-T_C)L^3}{\nu^2} = Gr\theta_i = Gr\frac{(T_i-T_C)}{(T_H-T_C)}. \tag{8}$$

Let Q represent the total heat flux across the enclosure. Then:

$$Q = h_C L(T_i - T_C) \tag{9}$$

where h_C is obtained using a standard correlation for an enclosure consisting of two isothermal vertical walls. A typical expression would be

$$Nu_C = \frac{h_C L}{k} = a(Gr_C)^b = aGr^b\theta_i^b \tag{10}$$

a and b being the constants in the correlation used.

The same heat flux Q must flow across the solid wall. Hence

$$Q = \frac{k_w K}{t}(T_H - T_i). \tag{11}$$

* Also referred to as the thermal resistance model [10].

Eliminating T_i between equations (9) and (11), the overall Nusselt number Nu can be obtained as

$$Nu = \frac{(Q/L)}{(T_H-T_C)}\frac{L}{k} = 1\bigg/\left(\frac{kt}{k_w L} + \frac{1}{Nu_C}\right). \tag{12}$$

Also, eliminating Q between equations (9) and (11) it follows that

$$\theta_i = 1\bigg/\left[1 + Nu_C\left(\frac{kt}{k_w L}\right)\right]. \tag{13}$$

Thus, the coupled equations (13) and (10) must be solved iteratively to obtain Nu_C and θ_i. Once Nu_C has been obtained, the overall Nusselt number can be calculated from equation (12).

The constants a and b to be used in correlation (10) are available in the literature. However, for numerical consistency, the values used were those which were generated by the present computations for the limiting case of the standard enclosure. These values are: $a = 0.1556$ and $b = 0.2843$.

Implications of the three wall conduction models

The difference between the three conduction models can be looked at in the following manner. Imagine the wall has different thermal conductivity $(k_w)_x$ and $(k_w)_y$ in the x and y directions, respectively. Then, the implications of the three wall conduction models are:

two-dimensional model	$(k_w)_x = (k_w)_y = k_w$
one-dimensional model	$(k_w)_x = k_w$; $(k_w)_y = 0$
lumped parameter approach	$(k_w)_x = k_w$; $(k_w)_y = \infty$.

The difference in the results obtained by the three models can be interpreted well in terms of the above implications.

Parameters of the problem

The complete conjugate problem, with two-dimensional wall conduction, is governed by four dimensionless parameters. These are the Grashof number Gr, the Prandtl number Pr, the dimensionless wall thickness t/L and the conductivity ratio k_w/k. The Prandtl number was kept fixed as 0.7 corresponding to air. The Grashof number was varied from 10^3 to 10^7.

For the one-dimensional and the lumped parameter wall conduction models, t/L and k_w/k do *not* appear as two separate parameters; instead, they appear only as one combination $k_w L/kt$. It is expected, therefore, that even for the complete conjugate analysis, an appropriate parameter should be $k_w L/kt$. The computed results support this choice; it is indeed found that for fixed $(k_w L/kt)$, the results of even the two-dimensional wall conduction model depend very little on t/L. The following values were considered: $k_w L/kt = 5$, 25, 50 and ∞, and $t/L = 0.2$ and 0.4.

COMPUTATIONAL PROCEDURE

The governing equations were solved numerically using the control-volume-based finite-difference method described by Patankar [17]. The application of the method to handle conjugate problems has been discussed in ref. [17] and, at greater length, in ref. [18]. The basic idea is to solve for the flow in the enclosure and the conduction in the wall simultaneously. This is achieved by taking the computational domain to include both the fluid and the solid regions. In the solid, the viscosity is assigned a very large value which makes the velocity zero there. The grid layout is such that the solid–fluid interface forms a control volume face for the neighboring grid points. Correct expressions for the heat flux (or, for the shear stress) across this interface are obtained by using the harmonic mean of the solid and fluid thermal conductivities (or, the harmonic mean of the viscosities).

An exponential differencing scheme is employed in the fluid. This reduces to the central difference type scheme in the solid where all the velocities are zero. Because of the nonlinearity of the momentum equations, the velocity–pressure coupling, and the coupling between the flow and the energy equation, an iterative solution scheme is necessary. In the present study the SIMPLER algorithm [17] was employed.

To obtain convergence at very high Grashof numbers, special under-relaxation procedures are necessary. In the present study, the inertial relaxation method of Ideriah [19] was used. A detailed summary of the effect of various underrelaxation parameters on the number of iterations required for convergence has been provided in ref. [20].

A 40×30 grid was used in all the computations. Of the 40 vertical grid lines, a disproportionate share of 10 grid lines were placed in the solid wall. The grid was packed close to the solid walls and the solid–fluid interface so that the boundary layer could be well resolved. The grid layout was chosen after a number of trial numerical experiments, the results of which were summarized in ref. [20]. For the case of an infinitely conducting wall, i.e. $(k_w L/kt) = \infty$, the grid layout which was finally chosen, yields an overall Nusselt number, which is within 2% of Caton's empirical correlation* in the range $(10^3 < Gr < 10^6)$ and within 6% at $Gr = 10^7$.

RESULTS

Streamline and isotherm plots

An appreciation for the nature of the flow and the temperature fields can be obtained by examining plots of the streamlines and isotherms. In all the figures that follow, the maximum value of the dimensionless streamfunction $\psi_{max}L^2/\nu$ is given in the figure captions. Different streamlines correspond to 0, $0.1\psi_{max}L^2/\nu$, $0.2\psi_{max}L^2/\nu$, $0.3\psi_{max}L^2/\nu$, etc. and different isotherms correspond to $\theta = 0, 0.1, 0.2, \ldots, 1$.

Figure 2 shows representative streamlines and isotherms for a Grashof number of 10^5. Panel (a) represents a poorly conducting wall and panel (b) represents an infinitely conducting wall, i.e. the standard enclosure with two isothermal vertical walls. The results of panel (a) correspond to a two-dimensional wall conduction model. The circulation pattern is counterclockwise, with flow downward at the cold left wall and upward at the hot right wall. Because of the temperature drop in the wall, the effective temperature difference driving the flow in panel (a) is less than that for panel (b); as a result, the strength of the flow, i.e. ψ_{max}, is less for case (a) than for case (b).

The temperature profile across the solid–fluid interface is quite non-uniform. This non-uniformity has a noticeable effect on the flow field; the flow in panel (a) is asymmetric whereas the flow for the isothermal walls shown in panel (b) is perfectly symmetric.

Figure 3 shows plots for the highest Grashof number studied, $Gr = 10^7$. A comparison is made for the streamlines and isotherms obtained using the two-dimensional and one-dimensional wall conduction models. As can be seen, the results for the two cases are nearly identical, supporting the conclusion that the one-dimensional approximation is a good substitute for the two-dimensional conjugate analysis.

Figure 4 also corresponds to $Gr = 10^7$. The effect of increasing the wall conductivity is examined. As expected, the two-dimensional wall effects diminish

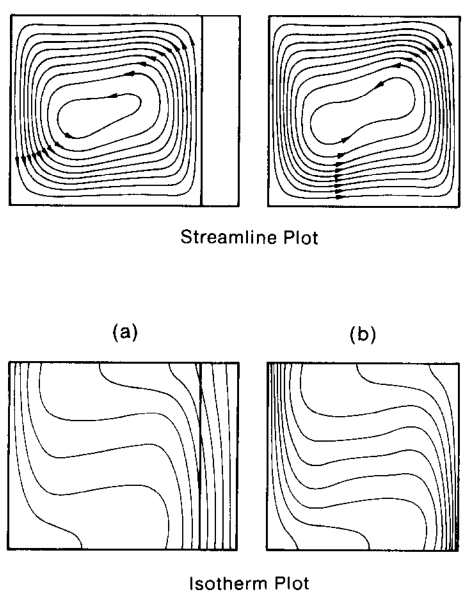

FIG. 2. Flow and temperature fields for $Gr = 10^5$ and $t/L = 0.2$. Panel (a) corresponds to two-dimensional wall conduction model with $(k_w L/kt) = 5$; and panel (b) is for isothermal walls $[(k_w L/kt) = \infty]$. The maximum streamfunction, $\psi_{max}L^2\nu$, is 10.4 for panel (a) and 12.6 for panel (b).

* $Nu = 0.15(Gr)^{0.29}$.

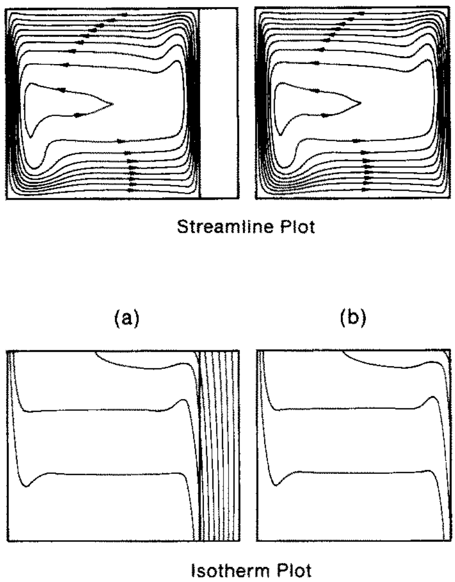

FIG. 3. Flow and temperature fields for $Gr = 10^7$, $(k_w L/kt) = 5$ and $t/L = 0.2$. Panel (a) two-dimensional wall conduction model; $\psi_{max} L^2/\nu = 26.7$. Panel (b) one-dimensional wall conduction model; $\psi_{max} L^2/\nu = 26.7$.

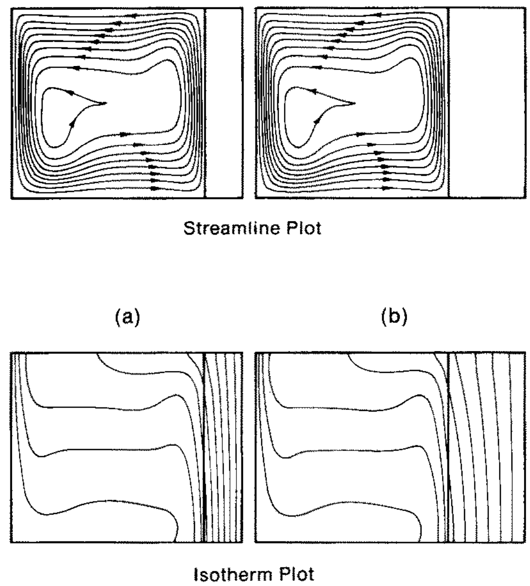

FIG. 5. Effect of t/L on the flow field. The plots correspond to $Gr = 10^6$ and are for two-dimensional wall conduction model. The conductance ratio, $(k_w L/kt) = 5$. Panel (a) corresponds to $t/L = 0.2$, and panel (b) to $t/L = 0.4$. The maximum streamfunction $\psi_{max} L^2/\nu = 10.4$ for panel (a) and 10.3 for panel (b).

(compare with Fig. 3, panel a) as the wall conductivity increases, and the flow tends to become more symmetric.

Finally, Fig. 5 has been prepared to examine the effect of t/L for a fixed value of $(k_w L/kt)$. The wall conduction model is, of course, two-dimensional.

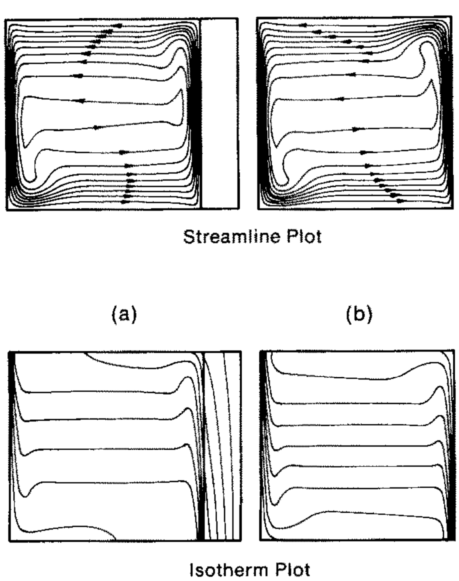

FIG. 4. Flow and temperature fields for $Gr = 10^7$ and $t/L = 0.2$. Panel (a) is for two-dimensional wall conduction model with $(k_w L/kt) = 25$, and panel (b) is for isothermal walls $[(k_w L/kt) = \infty]$. The maximum streamfunction, $\psi_{max} L^2/\nu$ is 33.7 for panel (a) and 40.6 for panel (b).

There are only slight differences in the streamline and isotherm plots for the two cases supporting the choice of $(k_w L/kt)$ as the appropriate non-dimensional parameter for this problem. This conclusion was typical of all the parametric cases studied in this investigation.

Temperature variation at the solid–fluid interface

The variation of the temperature at the solid–fluid interface is presented in Fig. 6. The solid curves correspond to the predictions of two- and one-dimensional wall conduction models; the results for these cases were too close to be resolved on the scale of Fig. 6. The dashed curves correspond to the uniform interface temperature as predicted by the lumped parameter analysis. For the two-dimensional wall conduction model, with a prescribed $(k_w L/kt)$, the results corresponding to $t/L = 0.2$ and $t/L = 0.4$ were found to be very close; hence, the solid curves in Fig. 6 represent both the t/L values.

Everything else remaining fixed, the effect of reducing $(k_w L/kt)$ is to decrease the interface temperature. This is expected; a reduction of $(k_w L/kt)$ implies a poorly conducting wall across which a greater temperature drop must occur.

For the conjugate case, both one-dimensional and two-dimensional, the interface temperature increases with the vertical distance. This is expected (recall Fig. 1 and the streamline plots of Figs. 2–5). The counter-clockwise rotating fluid becomes cold as it flows down past the left wall, and hence, it impinges at the bottom end of the right wall at a lower temperature making the interface temperature low there; as the fluid rises

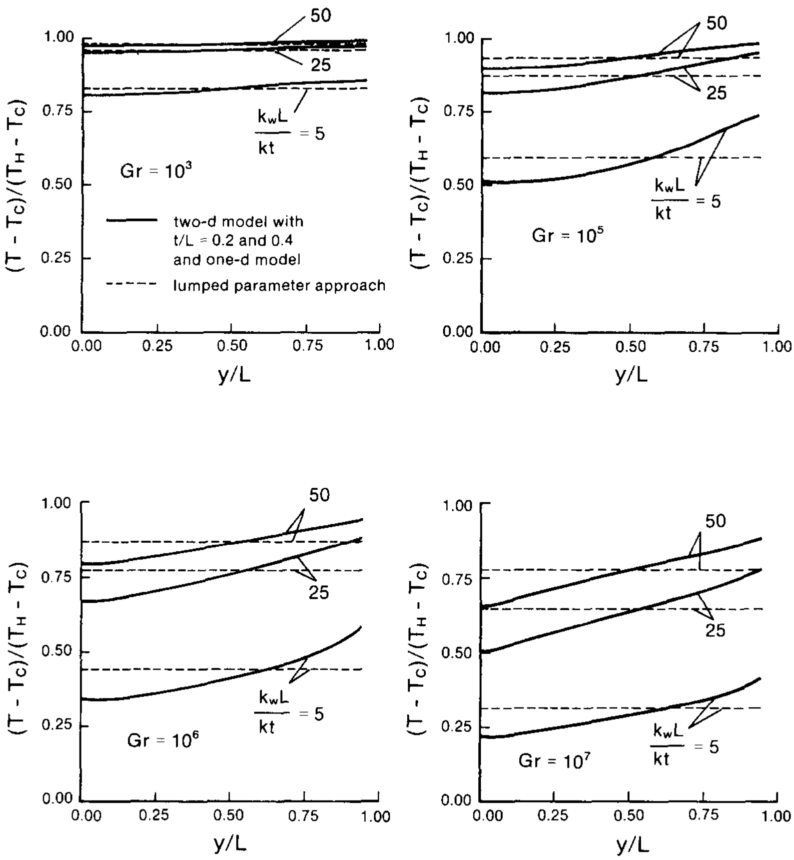

FIG. 6. Temperature variation at the solid–fluid interface.

up against the interface gaining heat from the wall, the temperature, expectedly, increases.

The uniform temperature at the interface as predicted by the lumped parameter approach can be understood, as discussed earlier, in terms of an implied infinite conductivity in the y direction. This uniform temperature appears, from Fig. 6, to be 'some sort of an average' of the non-uniform interface temperature predicted by the complete conjugate analysis; it is higher over the bottom half of the interface and lower in the upper half.

Variation of the heat flux at the solid–fluid interface

The variation of the local heat flux at the solid–fluid interface is plotted in Fig. 7. The results correspond to the two-dimensional wall conduction model. Again, the results for $t/L = 0.2$ and $t/L = 0.4$ for a fixed value of $(k_w L/kt)$, were too close to be resolved on the scale of Fig. 7.

The decrease in the local heat flux with increasing vertical distance is expected; it is a consequence of: (i) growing boundary-layer thickness at the solid–fluid interface as y increases, and (ii) increasing fluid temperature as the fluid moves up along the wall. The small decrease in heat flux with decreasing y near $y = 0$ is a local corner effect.

Comparing Figs. 6 and 7 it can be noted that cases involving a non-uniform interface temperature lead to a uniform interface flux and vice versa.

A comparison of the interface heat flux as predicted by the different wall conduction models is presented in Fig. 8. The results of the lumped parameter case correspond to an enclosure which is driven by a Grashof number, Gr, with an imposed temperature $\theta = 0$ at the left wall and $\theta = \theta_i$ at the right wall; θ_i being, of course, determined by the lumped parameter analysis. Compared to a conjugate analysis, the lumped parameter approach predicts a higher heat flux in the lower portion of the interface and a lower heat flux in the upper portion. This difference can be understood from Fig. 6 as being due to the predicted interface temperature, which is higher for the lumped parameter case in the bottom portion of the interface, and lower in the upper part.

The difference between the two-dimensional and the one-dimensional conjugate analyses lies in the fact that the former permits heat conduction in the wall in the y direction whereas the latter does not. As already noted, the temperature in the wall is increasing in the y direction. Hence, in a two-dimensional model, there must be a heat flow in the wall in the negative y direction which is expected to add onto and increase

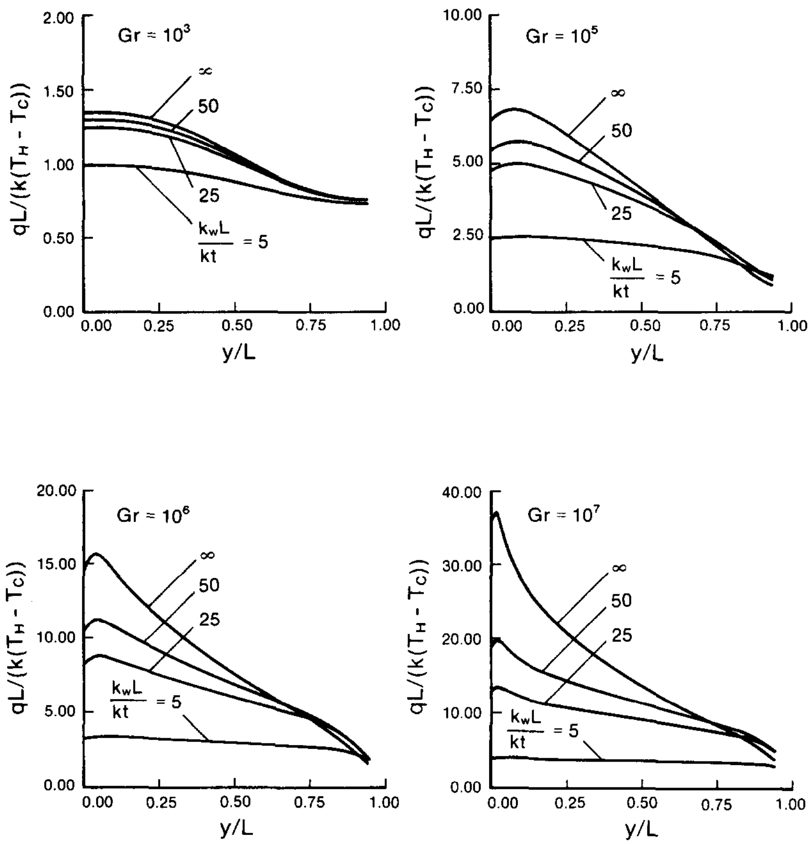

FIG. 7. Variation of the local heat flux at the solid–fluid interface. Results of the two-dimensional wall conduction model.

the interface flux near the bottom of the interface. As a result, it is expected that the local heat flux predicted by the two-dimensional model should be higher than that predicted by the one-dimensional model in the lower part of the interface, and smaller in the upper part. This is precisely what is predicted by the results shown in Fig. 8. The actual magnitude of the difference is, however, small.

Overall heat transfer results

The main quantity of practical interest is the total heat transfer Q across the enclosure. The total heat transfer may be expressed in terms of the average Nusselt number, given by

$$Nu = \frac{Q/L}{(T_H - T_C)}\frac{L}{k} = \frac{Q}{k(T_H - T_C)}. \tag{14}$$

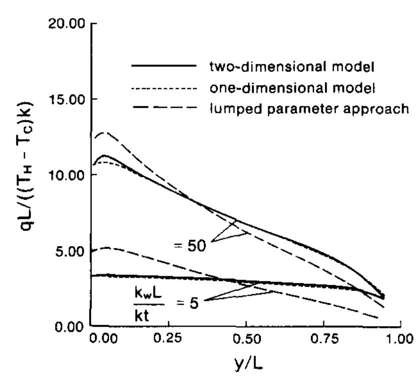

FIG. 8. Comparison of the local heat flux at the solid–fluid interface as predicted by different models; $Gr = 10^6$.

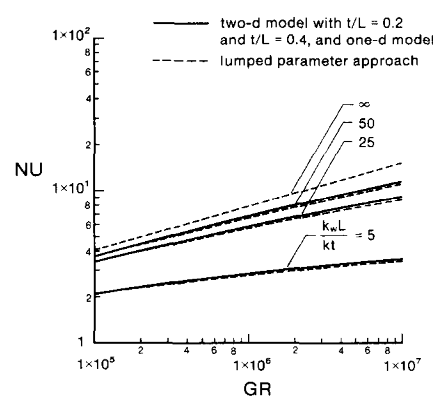

FIG. 9. Variation of the overall Nusselt number with Grashof number.

Table 1. Variation of the overall Nusselt number

Gr	$\frac{k_w L}{k_f t}$	Two-dimensional wall conduction $t/L = 0.2$	$t/L = 0.4$	One-dimensional wall conduction	Lumped parameter
10^3	5	0.87	0.87	0.87	0.84
	25	1.02	1.02	1.02	1.01
	50	1.04	1.04	1.04	1.04
	∞	1.06	1.06	1.06	1.07
10^5	5	2.08	2.08	2.08	2.05
	25	3.42	3.41	3.41	3.36
	50	3.72	3.71	3.71	3.67
	∞	4.08	4.08	4.08	4.05
10^6	5	2.87	2.87	2.87	2.77
	25	5.89	5.88	5.89	5.65
	50	6.81	6.80	6.81	6.56
	∞	7.99	7.99	7.99	7.86
5×10^6	5	3.35	3.35	3.35	3.25
	25	8.07	8.06	8.07	7.76
	50	9.86	9.85	9.85	9.53
	∞	12.50	12.50	12.50	12.52
10^7	5	3.53	3.53	3.53	3.43
	25	9.08	9.06	9.08	8.76
	50	11.39	11.38	11.39	11.07
	∞	15.09	15.09	15.09	15.29

For the one-dimensional and two-dimensional wall conduction models, Nu is obtained by the numerical integration of the local heat flux values; for the lumped parameter approach, Nu is obtained using equation (12).

Recall Fig. 8 in which the variation of local heat flux at the interface has been plotted. The overall Nusselt number Nu is merely the integral of the local heat flux with y (area under the curves). As can be seen, though the different models predict different local heat flux values, there is a trade-off in the integral sense—i.e. models which predict smaller values of the heat flux in the lower part of the interface yield higher values in the upper part and vice versa. Therefore, it may be expected that overall Nusselt number Nu should be close for the three different models. This expectation is confirmed by Fig. 9 in which the variation of Nu with Gr has been plotted. The solid curves represent the results of the two-dimensional model with $t/L = 0.2$ and $t/L = 0.4$ and the one-dimensional model (the differences being too small to be resolved on the scale of Fig. 9), and the dashed curves correspond to the lumped parameter approach. The numerical values of Nu are also listed in Table 1. As may be noted, the overall Nusselt number is predicted quite accurately by the one-dimensional model. In comparison, the lumped parameter model gives a slight under-prediction, but the difference is small ($\pm$3–4%).*

These overall Nusselt number predictions provide the most important result of the present study; it is interesting to find that despite their different physical implications, the overall heat transfer values are predicted quite well by the three different wall conduction models.

Consider the case of $k_w L/kt = \infty$ in Table 1. The values listed for the two-dimensional and one-dimensional models are those which were obtained by the numerical computations. From these values, a $Nu \sim Gr$ correlation was obtained using the least-squares fit method. The correlation so obtained gave $Nu = 0.1556\, Gr^{0.2843}$. This correlation was then used to process the lumped parameter analysis. It is for this reason that the Nu values for $k_w L/kt = \infty$ case are slightly different for the lumped model as compared to the one-dimensional and two-dimensional models, i.e. the difference is attributed to process of fitting the correlation.

It would have been desirable to develop a correlation for Nu as a function of Gr, kw/k and t/L, etc. This has not been done since the lumped model analysis agrees so well with the results of the complete conjugate case.

CONCLUSIONS AND RECOMMENDATIONS FOR FURTHER WORK

The present paper has dealt with a very basic conjugate natural convection heat transfer problem. Three different models to account for wall conduction have been examined: (i) the complete two-dimensional conjugate analysis; (ii) the one-dimensional wall conduction model; and (iii) the 'zeroth'-order lumped parameter approach. Results show that for

* The reader is warned that in the earlier version of this paper [21] the $Gr = 10^7$ results were not fully converged.

$Gr > 10^5$, the temperature distribution in the wall is quite two-dimensional, and the solid–fluid interface temperature is quite non-uniform. For the parametric range investigated, the overall heat transfer results of the three models are found to be quite close despite the different physical implications of these models. The local details predicted by the one-dimensional model are in close agreement with those of the two-dimensional model. Hence, the one-dimensional and lumped parameter network approaches are viable, quick, and economical alternatives to a complete two-dimensional analysis.

This study can now be extended to account for conduction in more than one wall. Again, the focus must be on comparing and identifying simpler one-dimensional and zero-dimensional type models which permit computation of important quantities of engineering interest more economically. Extension to three-dimensional enclosures and other geometries would be valuable, and so would be transient studies especially those which delineate the effect of wall conduction on flow stability.

REFERENCES

1. S. Ostrach, Natural convection in enclosures, *Adv. Heat Transfer* **8,** 161–227 (1972).
2. I. Catton, Natural convection in enclosures, *Proc. 6th Int. Heat Transfer Conference*, Toronto, Canada, pp. 13–19 (1978).
3. S. Ostrach, Natural convection heat transfer in cavities and cells, *Proc. 7th Int. Heat Transfer Conference*, Munich, F.R.G., Vol. 1, pp. 365–379 (1982).
4. J. W. Elder, Laminar free convection in a vertical slot, *J. Fluid Mech.* **23,** 77–98 (1965).
5. J. W. Elder, Turbulent free convection in a vertical slot, *J. Fluid Mech.* **23,** 99–111 (1965).
6. J. O. Wilkes, The finite difference computation of natural convection in an enclosed rectangular cavity. Ph.D. thesis, University of Michigan, Ann Arbor, MI (1963).
7. G. Z. Gershuni, E. M. Zhukhovitskii and E. L. Tarunin, *Mech. Liquids Gases, Akad. Sci. U.S.S.R.* No. 5, pp. 56–62 (1966).
8. G. de Vahl Davis, Laminar natural convection in a rectangular cavity, *Int. J. Heat Mass Transfer* **11,** 1675–1693 (1968).
9. I. P. Jones, A numerical study of natural convection in an air-filled cavity: comparison with experiment, *Numer. Heat Transfer* **2,** 193–213 (1979).
10. G. Lauriat, A numerical study of a thermal insulation enclosure: influence of the radiative heat transfer. In *Natural Convection in Enclosures*, ASME HTD-Vol. 8 (Edited by K. Torrance and I. Catton), pp. 63–71 (1980).
11. J. L. Balvanz and T. H. Kuehn, Effect of wall conduction and radiation on natural convection in a vertical slot with uniform heat generation on the heated wall. In *Natural Convection in Enclosures*, ASME HTD-Vol. 8 (Edited by K. Torrance and I. Catton), pp. 163–174 (1980).
12. D. W. Larson and R. Viskanta, Transient combined laminar free convection and radiation in a rectangular enclosure, *J. Fluid Mech.* **78,** 65–85 (1976).
13. D. M. Kim and R. Viskanta, Study of the effects of wall conductance on natural convection in differently oriented square cavities, *J. Fluid Mech.* **44,** 153–176 (1984).
14. D. M. Kim and R. Viskanta, Effect of wall heat conduction on natural convection heat transfer in a square enclosure, *J. Heat Transfer* **107,** 139–146 (1985).
15. D. M. Kim and R. Viskanta, Effect of wall conduction and radiation on natural convection in a rectangular cavity, *Numer. Heat Transfer* **7,** 449–470 (1984).
16. G. D. Mallinson, The effect of side wall conduction on natural convection in a slot, presented at the 22nd National Heat Transfer Conference, Niagara Falls, NY (1984).
17. S. V. Patankar, *Numerical Heat Transfer and Fluid Flow.* McGraw-Hill, New York (1981).
18. S. V. Patankar, A numerical method for conduction in composite materials, flow in irregular geometries, and conjugate heat transfer, *Proc. 6th Int. Heat Transfer Conference*, Toronto, Vol. 3, p. 279 (1978).
19. F. J. K. Ideriah, An inertial relaxation method of curing numerical instability in prediction of flows influenced by severe body forces, *J. mech. Engng Sci.* **22,** No. 3 (1980).
20. D. A. Kaminski, Analysis of natural convection flow in a square enclosure with complete account of conduction in one of the vertical walls. Ph.D. thesis, Rensselaer Polytechnic Institute (April 1985).
21. C. Prakash and D. A. Kaminski, Conjugate natural convection in a square enclosure: effect of conduction in one of the vertical walls. In *Heat Transfer in Enclosures*, ASME HTD-Vol. 39 (Edited by R. W. Douglass and A. F. Emery), pp. 49–54 (1984).

CONVECTION NATURELLE CONJUGUEE DANS UNE ENCEINTE CARREE: EFFET DE LA CONDUCTION DANS UNE DES PAROIS VERTICALES

Résumé—On étudie numériquement l'écoulement de convection naturelle stationnaire, laminaire dans une enceinte carrée. Une paroi verticale est épaisse, avec une conductivité thermique finie, tandis que les trois autres sont d'épaisseur nulle. Le problème est conjugué et l'attention est principalement portée sur l'effet de la conduction dans la paroi sur la convection dans l'enceinte. On étudie trois modèles séparés : (i) le cas conjugué complet dans lequel la conduction dans la paroi épaisse est supposée bidimensionnelle ; (ii) un modèle monodimensionnel dans lequel la conduction dans la paroi est supposée être dans la direction horizontale seule ; (iii) une approche qui suppose que la température de l'interface solide-fluide est uniforme. Un fluide de Boussinesq avec un nombre de Prandtl égal à 0,7 (air) est étudié pour des nombres de Grashof allant de 10^3 à 10^7. Pour des nombres de Grashof > 10^5, la distribution de température dans la paroi montre des effets bidimensionnels significatifs et la température d'interface solide–fluide est non uniforme. Cette non uniformité tend à rendre asymétrique la configuration d'écoulement dans la cavité. Dans le domaine étudié, les trois modèles prédisent à peu près la même valeur pour le transfert thermique global.

NATÜRLICHE KONVEKTION IN EINEM RECHTECKIGEN HOHLRAUM

Zusammenfassung—Es ist die stationäre, laminare, natürliche Konvektionsströmung in einer rechteckigen Kammer numerisch untersucht worden. Eine der vertikalen Kammerwände ist vergleichsweise dick bei endlicher Wärmeleitfähigkeit, während die Wandstärken der anderen drei Kammerwände vernachlässigbar sind. Das Hauptaugenmerk der Studie liegt auf der Untersuchung der Auswirkungen, die Leitungseffekte in der Wand auf Konvektionsströmungen in der Kammer haben. Drei unterschiedliche Modelle werden vorgestellt um Leitungsvorgänge in der Wand zu untersuchen: (1) der Fall, bei dem vollständige zweidimensionale Wärmeleitung in der dicken senkrechten Wand angenommen wird, (2) ein eindimensionales Modell, bei dem Leitung nur in horizontaler Richtung angenommen wird, (3) eine Untersuchung mit konzentrierten Parametern bei der gleichmäßige Grenzflächentemperaturen zwischen Feststoff und Fluid vorausgesetzt werden. Ein Boussinesq-Fluid mit einer Prandtl-Zahl von 0,7 (Luft) und Grashof-Zahlen im Bereich von 10^3 bis 10^7 wurde verwendet. Bei Grashof-Zahlen größer als 10^5 traten typische zwei-dimensionale Temperaturverteilungen in der Wand auf, bei der die Grenzflächentemperatur zwischen Festkörper und Fluid recht uneinheitlich war. Diese Ungleichförmigkeit ruft wohl die asymmetrische Strömungsform in dem Hohlraum hervor. Im untersuchten Parameterbereich liefern alle drei Modelle nahezu den gleichen Wert für den Gesamtwärmeübergang.

СОПРЯЖЕННАЯ ПОСТАНОВКА ЗАДАЧИ О ЕСТЕСТВЕННОЙ КОНВЕКЦИИ В ПРЯМОУГОЛЬНОМ ЗАМКНУТОМ ОБЪЕМЕ: ЭФФЕКТ ТЕПЛОПРОВОДНОСТИ ОДНОЙ ИЗ ВЕРТИКАЛЬНЫХ СТЕНОК

Аннотация—Численно анализируется устойчивая ламинарная естественная конвекция в прямоугольном объеме. Одна вертикальная стенка полости толстая, имеющая конечное значение теплопроводности, в то время как толщины трех остальных считаются нулевыми. Основная цель сопряженной постановки задачи—исследование влияния теплопроводности в стенке на естественную конвекцию в полости. Рассматриваются три различных модели теплопроводности стенки: (i) полностью сопряженный случай, когда теплопроводность в толстой вертикальной стенке предполагается двумерной; (ii) одномерная модель теплопроводности в стенке с переносом тепла только в горизонтальном направлении; и (iii) модифицированный параметрический подход, предполагающий однородность температуры на границе раздела твердое тело-жидкость. Исследования проводятся в приближении Буссинеска для воздуха с числом Прандтля 0,7 и числами Грасгофа в диапазоне от 10^3 до 10^7. Для $Gr > 10^5$ распределение температуры в стенке является существенно двумерным, а температура на границе раздела твердое тело-жидкость существенно неоднородной. Из-за отмеченной неоднородности режим течения в полости трансформируется на асимметричный. В исследуемом диапазоне параметров все три модели предсказывают почти одно и то же значение суммарного коэффициента теплообмена.